NEUROPATHOLOGY

Neuropathology 2015; ••, ••–•• doi:10.1111/neup.12280

Case Report

Familial idiopathic basal ganglia calcification: Histopathologic features of an autopsied patient with an *SLC20A2* mutation

Tadashi Kimura,[1] Takeshi Miura,[2,4] Kenju Aoki,[4] Shoji Saito,[5] Hiroaki Hondo,[5] Takuya Konno,[2] Akio Uchiyama,[6] Takeshi Ikeuchi,[3] Hitoshi Takahashi[1] and Akiyoshi Kakita[1]

Departments of [1]Pathology, [2]Neurology and [3]Molecular Genetics, Brain Research Institute, University of Niigata, Niigata, Departments of [4]Neurology, [5]Neurosurgery, and [6]Pathology, Toyama Prefectural Central Hospital, Toyama, Japan

Idiopathic basal ganglia calcification (IBGC), or Fahr's disease, is a neurological disorder characterized by widespread calcification in the brain. Recently, several causative genes have been identified, but the histopathologic features of the brain lesions and expression of the gene products remain unclear. Here, we report the clinical and autopsy features of a 62-year-old Japanese man with familial IBGC, in whom an *SLC20A2* mutation was identified. The patient developed mild cognitive impairment and parkinsonism. A brain CT scan demonstrated abnormal calcification in the bilateral basal ganglia, thalami and cerebellum. An MRI study at this point revealed glioblastoma, and the patient died 6 months later. At autopsy, symmetric calcification in the basal ganglia, thalami, cerebellar white matter and deeper layers of the cerebral cortex was evident. The calcification was observed in the tunica media of small arteries, arterioles and capillaries, but not in veins. Immunohistochemistry using an antibody against type III sodium-dependent phosphate transporter 2 (PiT-2), the *SLC20A2* product, demonstrated that astrocytic processes were labeled in several regions in control brains, whereas in the patient, reactivity in astrocytes was apparently weak. Immunoblotting demonstrated a marked decrease of PiT-2 in the patient. There are few autopsy reports of IBGC patients with confirmation of the genetic background. The autopsy features seem informative for better understanding the histogenesis of IBGC lesions.

Key words: Fahr's disease, idiopathic basal ganglia calcification, PiT-2, primary familial brain calcification, SLC20A2.

INTRODUCTION

Idiopathic basal ganglia calcification (IBGC), also known as Fahr's disease or primary familial brain calcification, is a psychoneurological disorder characterized by symmetrical calcification in the basal ganglia and other brain regions. It is usually sporadic, but occasionally familial. Clinically, patients with IBGC may suffer from movement disorder, and cognitive and cerebellar impairment, but some patients may be asymptomatic.[1] As well as in IBGC, brain calcification can also occur in individuals with several etiologically distinct conditions, including infectious, metabolic, mitochondrial and hereditary disorders, and even during normal ageing, the age at onset, manifestations and clinical courses showing wide variation.[2] Therefore, diagnosis of IBGC relies on the absence of such conditions.

Genetic analysis of IBGC families with autosomal dominant inheritance has revealed five implicated chromosomal regions: IBGC1-5.[3–5] In 2012 Wang *et al.* reported an *SLC20A2* gene mutation at IBGC3 in a large Chinese family[6] and thereafter many other mutations in the gene were found in over 40 families worldwide.[7–9] The *SLC20A2* encodes type III sodium-dependent phosphate transporter 2 (PiT-2). Therefore, it has been speculated that a loss of function of phosphate-calcium metabolism may be associated with the abnormal calcification. In the following year, mutations in two novel causative genes were also identified – *PDGFRB* at IBGC4[10–12] and *PDGFB* at IBGC5[13–15] – which encode platelet-derived growth factor receptor-β (PDGFRB) and its ligand platelet-derived growth factor-β (PDGFB), respectively. Recently, a mutation in a novel causative gene, *XPR1* gene, which encodes a retroviral receptor with phosphate export function, was identified in a North American family with IBGC of Swedish ancestry.[16] As yet, no potentially implicated genes at IBGC1 on chromosome 14q and IBGC2 on chromosome 2q37 have been identified.

Correspondence: Akiyoshi Kakita, MD, PhD, Department of Pathology, Brain Research Institute, University of Niigata, 1 Asahimachi, Chuo-ku, Niigata 951-8585, Japan. Email: kakita@bri.niigata-u.ac.jp

Received 7 October 2015; revised and accepted 10 November 2015.

In 2014, a clinico-genetic study in Japan identified five families and two sporadic patients with *SLC20A2* mutations.[17] This study demonstrated that the frequency of *SLC20A2* mutations in familial IBGC[17] appeared to be as high in Japan as in other countries.[8]

In general, IBGC is not a critical condition for individuals affected, and consequently only a small number of autopsy reports of IBGC patients have been available.[18–23] Here, we report the histopathological features and PiT-2 expression in the brain of an autopsied Japanese man with familial IBGC, in whom an *SLC20A2* mutation was identified.

CLINICAL SUMMARY

A 62-year-old Japanese man, a carpenter, with a medical history of diabetes mellitus and cerebral lacunar infarction, developed difficulty in driving a car, and subsequently retired from his job in August 2012. In November of the same year, he was transported to the Emergency Department of a local hospital after falling from a ladder. A CT scan taken at the hospital revealed abnormal calcification in the brain, and therefore he was referred to the Department of Neurology, Toyama Prefectural Hospital. Although he had experienced no problems with daily life activities, a neurological examination revealed cognitive impairment (Hasegawa dementia scale revised: 14/30 points) and parkinsonism, including a masked face, weak voice, bradykinesia and lead-pipe rigidity of the extremities. A retrospective survey of CT images, taken 10 years previously in 2002, when the patient had been diagnosed as having cerebral infarction, revealed that calcification had already been present in the bilateral basal ganglia, thalami, and cerebral cortex and white matter (Fig. 1A–C). The new CT images demonstrated much more obvious calcification, which had spread to the cerebellar white matter and dentate nucleus (Fig. 1D–F). Anamnesis revealed that various members of the patient's family (Fig. 2A), including his mother (I-2), two brothers (II-1 and II-4), a niece (III-1) and a nephew (III-6), had suffered from brain calcification, and that his mother and an elder brother had been diagnosed as having dementia and Parkinson's disease, respectively. A diagnosis of familial IBGC was made. One month later, there was deterioration of the patient's ability to stand up and remain standing, and therefore he was readmitted in a slightly drowsy state. A brain MRI study demonstrated a tumorous lesion involving the left frontal lobe, thalamus, midbrain and pons. A biopsy sample was obtained from the left frontal lesion, and histopathological examination demonstrated glioblastoma. The patient received palliative therapy only and died in February 2013.

A general autopsy was performed, at which time the brain weighed 1170 g, and this revealed a glioblastoma involving the corpus callosum, septum pellucidum, white

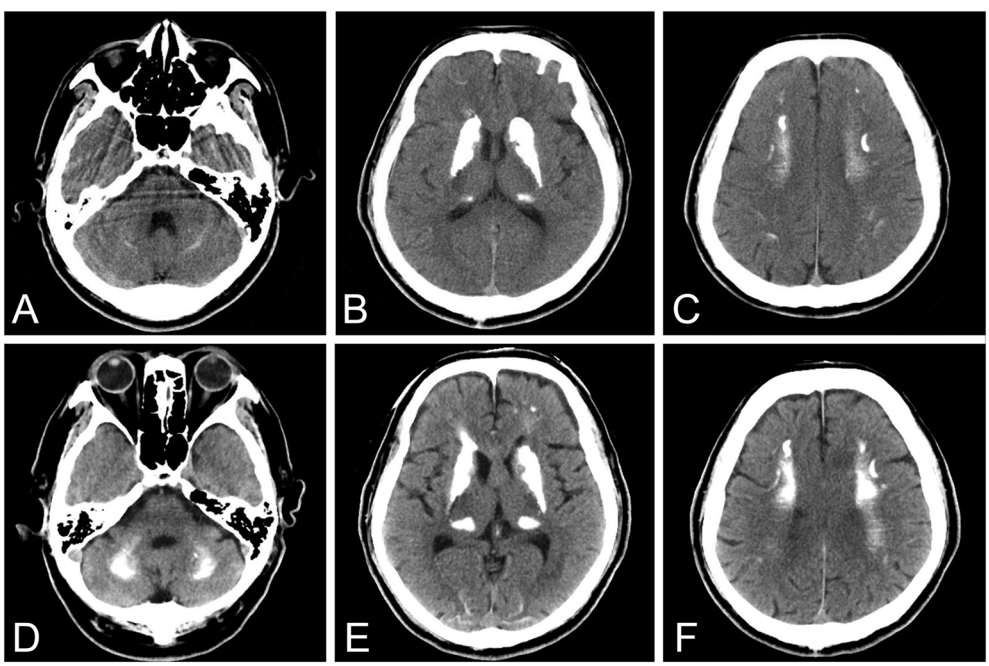

Fig. 1 Axial CT scans taken in 2002 (A-C) and 2012 (D-F) through the pons and cerebellum (A, D), basal ganglia (B, E), and centrum semiovale (C, F), demonstrating bilaterally symmetrical high-intensity lesions suggestive of calcification involving the basal ganglia, pulvinar, cerebellar dentate nucleus, and cerebral cortex. Note that the calcification becomes much more marked with the passage of time in these lesions, including the cerebellar (D) and cerebral white matter (F) and occipital cortex (E).

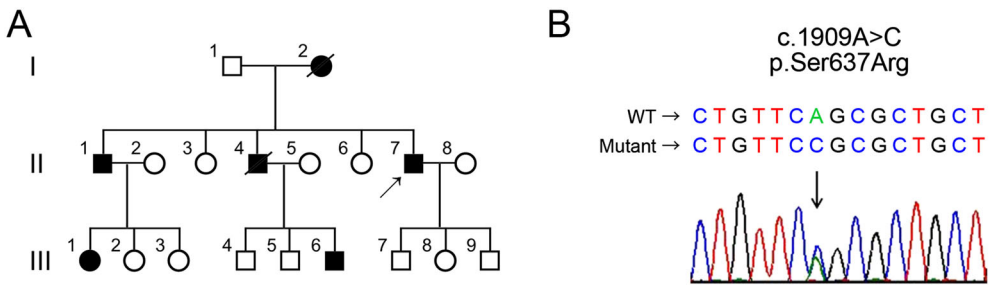

Fig. 2 (A) Family tree of the present patient (arrow). Members indicated by filled symbols had brain calcification. (B) A missense mutation in the *SLC20A2* gene.

matter close to the lateral ventricle, caudate nucleus, putamen, globus pallidus, thalamus, amygdala, tegmentum of the midbrain and pons, and cerebellum. Histologically, the tumor consisted of pleomorphic astrocytic cells with microvascular proliferation.

METHODS

The present study was approved by the Ethics Committee of Niigata University. Written informed consent for autopsy, collection of samples and their subsequent use for genetic analysis and other research purposes was obtained from the patient's next of kin, and further written informed consent was obtained from the patient's elder brother for genetic analysis of blood samples taken from him.

The brain and spinal cord were fixed in phosphate-buffered 20% formalin, and multiple tissue blocks were embedded in paraffin. Histological examination was performed on 4-μm-thick sections stained with HE, KB, Elastica-Goldner stain, PAS, Berlin Blue stain for iron and von Kossa stain for calcium. Selected sections were immunostained with antibodies against phosphorylated α-synuclein (pα-Syn) (monoclonal; pSyn #64; Wako, Osaka, Japan; diluted 1:10000, after pretreatment with formic acid for 5 min), β-amyloid (monoclonal; 6F/3D; Dako, Glostrup, Denmark; 1:50), phosphorylated tau (p-Tau) (monoclonal; clone AT8; Fujirebio Europe N.V., Gent, Belgium; 1:200), and PiT-2 (polyclonal, Atlas Antibodies, Stockholm, Sweden; 1:50, after autoclaving for 10 min at 121°C in 10 mmol/L sodium citrate buffer). As a control, formalin-fixed, paraffin-embedded sections from six patients (four male aged 62, 76, 77 and 78 years, and two female aged 60 and 79 years) without neurological disorders were used.

Protein extracted from fresh-frozen samples of the frontal cortex, putamen and cerebellar white matter of the present patient was used as previously described.[24] As controls, frozen tissue samples from four patients without any neurological disorders (three male aged 71, 77 and 78 years, and one female aged 79 years) were used. Tissue lysates were separated in 10% sodium dodecyl sulfate polyacrylamide gel and subjected to immunoblotting using the anti-PiT-2 antibody and an anti-β-actin antibody (monoclonal, Sigma, St Louis, MO, USA; 1:20000) as previously described.[25]

Genomic DNA was extracted from the patient's fresh-frozen frontal cortex tissue and a sample of whole blood from his elder brother. Mutational analysis of *SLC20A2* was performed by Sanger sequencing of all coding regions, using methods described elsewhere.[26]

RESULTS

SLC20A2 gene analysis

A heterozygous substitution, c.1909A > C (p.Ser637Arg) in exon 11 of *SLC20A2*, was identified in both the patient and his brother (Fig. 2B). The mutation was identical to that of three individuals of two Japanese families previously reported.[17]

Pathology

The cut surfaces of the caudate nucleus, putamen, globus pallidus and thalamus exhibited brownish discoloration and a gritty consistency (Fig. 3A) due to multiple foci of calcification, forming coarse and oval-shaped deposits with a variety of sizes, within the brain parenchyma and blood vessel walls (Fig. 3B,C). Within the lesions, gliosis was evident. Similar, but less severe calcification was also observed in deeper layers of the cerebral cortex at the depth of a sulcus (Fig. 3D) and in the pulvinar (Fig. 3E). In the cerebellum, marked brownish discoloration was seen in and around the dentate nucleus (Fig. 3F). Calcification in the dentate nucleus itself was relatively mild (Fig. 3G), whereas it was much more severe in the white matter nearby and the granule cell layer close to the deep white matter (Fig. 3H).

In these lesions, calcification was observed in the tunica media of medium- and small-caliber arteries, arterioles and capillaries (Fig. 3I). A small number of arteries exhibited severe calcification that had resulted in obstruction of the lumen (Fig. 3J). The deposited materials were stained with von Kossa (Fig. 3K), Berlin blue (Fig. 3L) and PAS (not

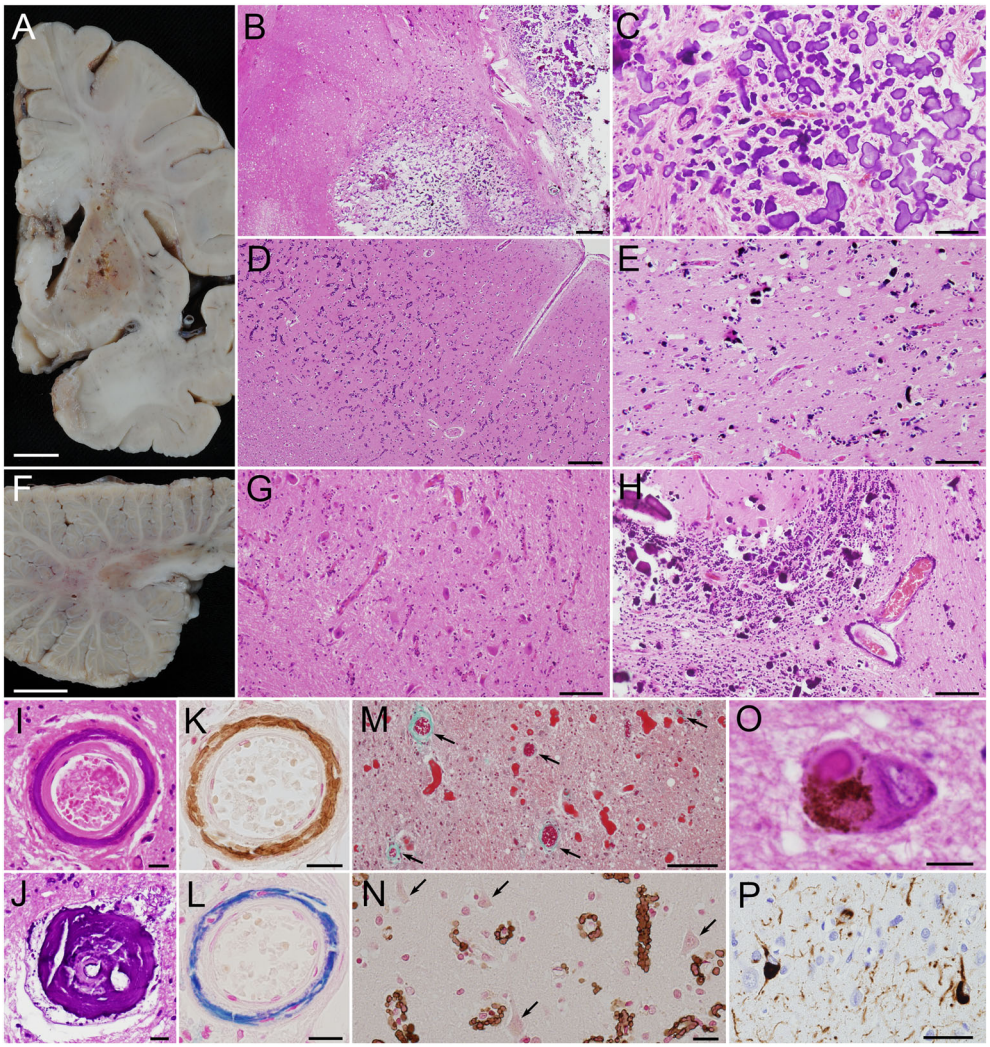

Fig. 3 Autopsy findings. (A) Coronally cut surface of the cerebrum showing brownish discoloration in the putamen, globus pallidus, caudate nucleus and deep white matter. (B-E) Microscopic features of the cerebrum. (B) A low-magnification view demonstrates multiple foci of calcification in the putamen (right) and globus pallidus (center). (C) A higher-magnification view of the globus pallidus showing coarse calcium deposition. Calcification in deeper layers of the occipital cortex at the depth of a sulcus (D) and the pulvinar (E). (F) Sagittally cut surface of the cerebellum showing discoloration in the dentate nucleus and white matter. In contrast to mild calcification in the dentate nucleus (G), severe calcification in the white matter and granule cell layer is evident (H). (I-L) Higher-magnification views demonstrating mineralization in the vessel walls. Mineralization in the tunica media of a small-sized artery (I) and in the wall and lumen of a vessel (J), containing hydroxyapatite (K) and iron (L). (M, N) Even in severely mineralized lesions, vessels without apparent deposition (arrows in M) and normal-looking neurons (arrows in N) are evident. (O) A Lewy body in the substantia nigra. (P) Several neurofibrillary tangles and threads in the temporal neocortex. HE (B-E, G-J and O), von Kossa (K and N), Berlin Blue (L) and Elastica-Goldner (M) stain. (P) P-Tau immunohistochemistry. Bar = 1 cm (A and F), 500 μm (B), 100 μm (C, E, G, H and M), 200 μm (D), 20 μm (I-L, N and P), and 10 μm (O).

shown), indicating that they contained calcium, iron and glycogen (glycosylated sugars / proteins), respectively. Veins were seldom affected. Even within areas showing marked calcification, some arteries without calcification (Fig. 3M) and scattered normal-looking neurons (Fig. 3N) were evident.

Neuronal loss with pα-Syn-immunolabeled Lewy bodies and neurites was evident in the substantia nigra (Fig. 3O), locus ceruleus, dorsal vagal nucleus, olfactory bulb, sympathetic ganglia and amygdala, leading to a diagnosis of Parkinson's disease. P-Tau immunohistochemistry demonstrated neurofibrillary tangles and neuropil threads, restricted to the hippocampus (Fig. 3P), and the temporal and frontal cortex. No β-amyloid deposits or argyrophilic grains were observed. In the visceral organs, no abnormal calcification was observed.

PiT-2 immunohistochemistry

In control brains, intense PiT-2 immunoreactivity was observed in layers II/III of the cerebral cortex (Fig. 4A),

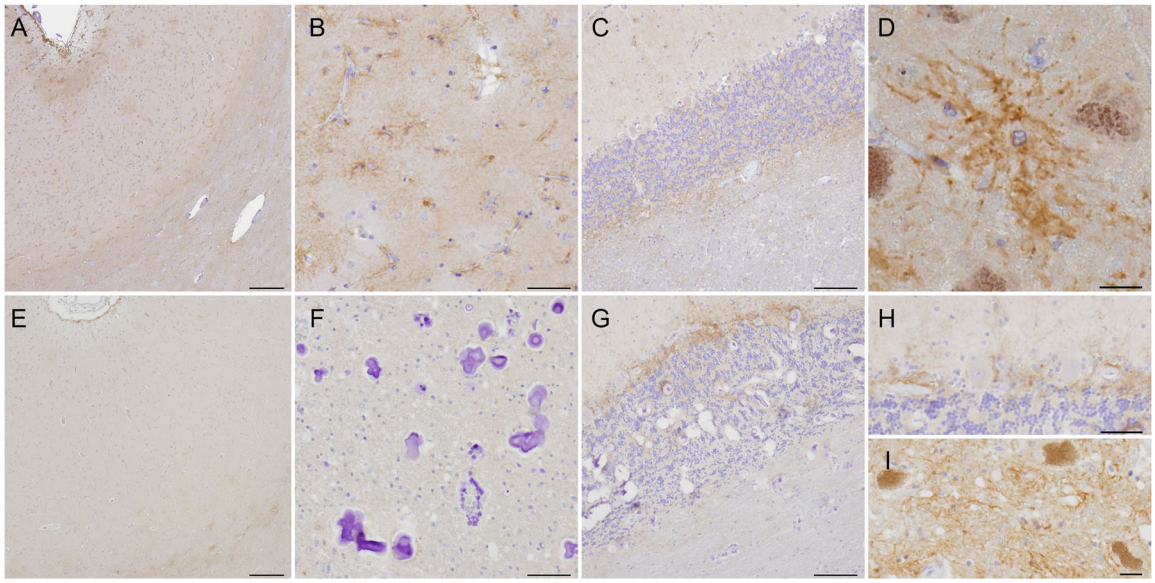

Fig. 4 Type III sodium-dependent phosphate transporter 2 (PiT-2) immunohistochemistry. Images of the frontal cortex (A, E), putamen (B, F) and cerebellum (C, G) of the controls (A-D), and the present patient (E-I). Note presence of reactivity in the controls, but not in the patient. (D) A higher-magnification view of the putamen demonstrating reactivity in the astrocytic processes. Reactivity in the Purkinje cell layer (H) and substantia nigra (I). Bar = 200 μm (A and E), 50 μm (B and F), 100 μm (C, G and H) and 20 mm (D and I).

putamen (Fig. 4B), and the border areas between the cerebellar granule cell layer and the adjacent white matter (Fig. 4C), where astrocytic processes (Fig. 4D) extending to the blood vessels and pia mater were labeled.

In the present patient, PiT-2 immunoreactivity in the cerebral cortex (Fig. 4E), putamen (Fig. 4F) and cerebellar white matter (Fig. 4G) was weaker than that of the controls. However, fine structures, presumably corresponding to astrocytic processes in the Purkinje cell layer (Fig. 4H) and substantia nigra (Fig. 4I) were also labeled.

Western blotting

Abundant PiT-2 expression was evident in all tissues from the controls, whereas markedly faint expression of the protein was detected in tissues from the patient (Fig. 5).

DISCUSSION

In this patient with familial IBGC, we identified a *SLC20A2* mutation (Fig. 2) and a marked decrease of PiT-2 expression in the brain lesions (Figs 4,5). Also, we studied some histopathological pictures that appeared to be informative for better understanding the histogenesis of the lesions.

Previous examinations of brain lesions in sporadic,[18] familial[19–22] and infant[23] cases of IBGC have commonly identified calcification within and around the vessel walls in the basal ganglia, thalamus, deeper layers of the cerebral cortex and cerebellar white matter. In the present patient, the distribution pattern of calcification appeared to be consistent with those of previous cases. Brain CT images taken after an interval of 10 years indicated that calcification had become much more marked with the passage of time, especially in the cerebellar white matter (Fig. 1). At present, it is unclear why these specific anatomical regions are vulnerable in IBGC. These vulnerable regions are supplied by long-perforating branches that arise from, and then run

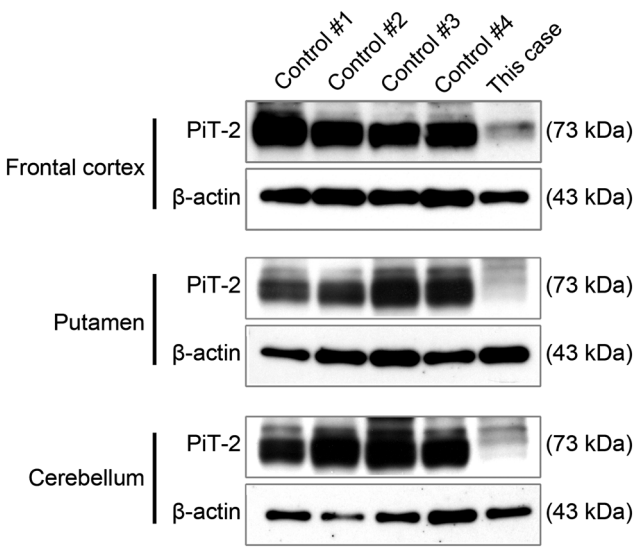

Fig. 5 Type III sodium-dependent phosphate transporter 2 (PiT-2) expression in autopsied tissue. Samples were collected from the frontal cortex, putamen and cerebellum of four controls and the present patient. Abundant expression of PiT-2 (73 kDa) is detected in the controls, whereas only faint expression is observed in the sample from the patient.

perpendicular to, major arteries,[27] for example, the lateral striate arteries arising from the middle cerebral artery. The hemodynamics of such anatomically characteristic arteries and arterioles[28] might have some association with the calcification.

It was evident that calcification was associated with the vessel walls (Fig. 3I–M), and even though some vessels showed stenosis or obstruction of their lumina (Fig. 3J), the morphology of neurons within these lesions was preserved (Fig. 3N). This suggests that the calcification itself does not always cause ischemic damage to the brain parenchyma around the affected vessels. This notion may be consistent with the clinical manifestations of the IBGC, which show a wide range from asymptomatic to variably symptomatic. Moreover, as demonstrated in the present case and a previous report,[29] the deposited materials contained hydroxyapatite (Fig. 3K), iron (Fig. 3L), zinc, magnesium and other trace heavy metals, and glycogen (glycosylated sugars / proteins); therefore the phenomenon could be regarded as "mineralization" in the strict sense rather than mere "calcification".

Information on the causative genes and expression of their products would be useful for better understanding the pathomechanisms of IBGC. In mouse brain, expression of PiT-2 is detectable immunohistochemically in vascular endothelial cells, neurons and astrocytes.[30] Interestingly, *slc20a2* homozygous knockout mice exhibit irregular calcification in the bilateral thalami, basal ganglia, and cerebral cortex, but not in the cerebellum.[31] This distribution pattern sparing the cerebellum appears similar to that in the present patient. However, even in our patient, cerebellar calcification developed later (Fig. 1), and therefore this tendency might also apply to knockout mice.

According to a mRNA profiling study on human tissue, *SLC20A2* mRNA was expressed ubiquitously but at a much higher level in skeletal muscles.[32] A more recent genetic study using the Allen Institute Human Brain Atlas Resources demonstrated the *SLC20A2* gene expression pattern in the human brain in detail, the expression being relatively high in the globus pallidus, thalamus and cerebellum.[33] Such a gene expression pattern is similar to the pattern of calcification we observed in the present patient. Our immunohistochemical study of control brains confirmed the expression of PiT-2 protein in these regions (Fig. 4A–D). Moreover, we confirmed a marked decrease of PiT-2 in brain lesions of the patient using immunohistochemistry and Western blotting (Figs 4,5), consistent with the notion that the *SLC20A2* mutation leads to loss of function of the product. Furthermore, we observed PiT-2 expression in the astrocytes of control brains (Fig. 4D), in contrast to decreased expression in our patient (Fig. 4E–G). Therefore, astrocyte dysfunction associated with loss of PiT-2 might alter local metabolism involving calcium and other metals. However, the mechanistic association between the decrease of PiT-2 and vascular calcification still remains unclear. Moreover, the significance of the unexpected expression of PiT-2 in several brain regions (Fig. 4H,I) remains unexplained.

Diffuse neurofibrillary tangles with calcification (DNTC) is a neurological disorder characterized by fronto-temporal lobar atrophy with widespread calcification and numerous neurofibrillary tangles, but without senile plaques.[34,35] The distribution pattern of the calcification is similar to that of IBGC, and therefore it has been discussed whether DNTC and IBGC belong to a single disease entity. It is unlikely that the present case would be regarded as DNTC, because neurofibrillary tangles were limited in both number and distribution (Fig. 3P). The presence of Lewy bodies and neurites (Fig. 3O) seems to be a feature of DNTC[36] rather than IBGC. However, at present, it is unclear whether this finding is merely coincidental, or whether it has certain associations with the pathomechanisms underlying IBGC.

Our present report, for the first time, has provided evidence for PiT-2 expression in a patient with genetically confirmed IBGC. Further studies will be needed to clarify the pathomechanisms underlying the calcification in IBGC.

REFERENCES

1. Manyam BV. What is and what is not 'Fahr's disease'. *Parkinsonism Relat Disord* 2005; **11**: 73–80.
2. Bonazza S, La Morgia C, Martinelli P, Capellari S. Striopallido-dentate calcinosis: a diagnostic approach in adult patients. *Neurol Sci* 2011; **32**: 537–545.
3. Geschwind DH, Loginov M, Stern JM. Identification of a locus on chromosome 14q for idiopathic basal ganglia calcification (Fahr disease). *Am J Hum Genet* 1999; **65**: 764–772.
4. Volpato CB, De Grandi A, Buffone E *et al.* 2q37 as a susceptibility locus for idiopathic basal ganglia calcification (IBGC) in a large South Tyrolean family. *J Mol Neurosci* 2009; **39**: 346–353.
5. Dai X, Gao Y, Xu Z *et al.* Identification of a novel genetic locus on chromosome 8p21.1-q11.23 for idiopathic basal ganglia calcification. *Am J Med Genet B Neurospychiatr Genet* 2010; **153B**: 1305–1310.
6. Wang C, Li Y, Shi L *et al.* Mutations in SLC20A2 link familial idiopathic basal ganglia calcification with phosphate homeostasis. *Nat Genet* 2013; **44**: 254–256.
7. Zhang Y, Guo X, Wu A. Association between a novel mutation in SLC20A2 and familial idiopathic basal ganglia calcification. *PLoS One* 2013; **8**: e57060.
8. Hsu SC, Sears RL, Lemos RR *et al.* Mutations in SLC20A2 are a major cause of familial idiopathic basal ganglia calcification. *Neurogenetics* 2013; **14**: 11–22.

9. Westenberger A, Klein C. The genetics of primary familial brain calcifications. *Curr Neurol Neurosci Rep* 2014; **14**: 490.
10. Nicolas G, Pottier C, Maltête D *et al.* Mutation of the PDGFRB gene as a cause of idiopathic basal ganglia calcification. *Neurology* 2013; **80**: 181–187.
11. Nicolas G, Pottier C, Charbonnier C *et al.* Phenotypic spectrum of probable and genetically-confirmed idiopathic basal ganglia calcification. *Brain* 2013; **136**: 3395–3407.
12. Sánchez-Contreras M, Baker MC, Finch NA *et al.* Genetic screening and functional characterization of PDGFRB mutations associated with basal ganglia calcification of unknown etiology. *Hum Mutat* 2014; **35**: 964–971.
13. Keller A, Westenberger A, Sobrido MJ *et al.* Mutations in the gene encoding PDGF-B cause brain calcifications in humans and mice. *Nat Genet* 2013; **45**: 1077–1082.
14. Nicolas G, Jacquin A, Thauvin-Robinet C *et al.* A de novo nonsense PDGFB mutation causing idiopathic basal ganglia calcification with laryngeal dystonia. *Eur J Hum Genet* 2014; **22**: 1236–1238.
15. Nicolas G, Rovelet-Lecrux A, Pottier C *et al.* PDGFB partial deletion: a new, rare mechanism causing brain calcification with leukoencephalopathy. *J Mol Neurosci* 2014; **53**: 171–175.
16. Legati A, Giovannini D, Nicolas G *et al.* Mutations in *XPR1* cause primary familial brain calcification associated with altered phosphate export. *Nat Genet* 2015; **47**: 579–581.
17. Yamada M, Tanaka M, Takagi M *et al.* Evaluation of SLC20A2 mutations that cause idiopathic basal ganglia calcification in Japan. *Neurology* 2014; **82**: 705–712.
18. Kobayashi S, Yamadori I, Miki H, Ohmori M. Idiopathic nonarteriosclerotic cerebral calcification (Fahr's disease): an electron microscopic study. *Acta Neuropathol* 1987; **73**: 62–66.
19. Miklossy J, Mackenzie IR, Dorovini-Zis K *et al.* Severe vascular disturbance in a case of familial brain calcinosis. *Acta Neuropathol* 2005; **109**: 643–653.
20. Wszolek ZK, Baba Y, Mackenzie IR *et al.* Autosomal dominant dystonia-plus with cerebral calcifications. *Neurology* 2006; **67**: 620–625.
21. Wider C, Dickson DW, Schweitzer KJ, Broderick DF, Wszolek ZK. Familial idiopathic basal ganglia calcification: a challenging clinical-pathological correlation. *J Neurol* 2009; **256**: 839–842.
22. Larsen TA, Dunn HG, Jan JE, Calne DB. Dystonia and calcification of the basal ganglia. *Neurology* 1985; **35**: 533–537.
23. Matsui K, Yamada M, Kobayashi T *et al.* An autopsy case of Fahr disease (infantile form). *No To Hattatsu* 1992; **24**: 358–363. in Japanese.
24. Kaneko H, Kakita A, Kasuga K *et al.* Enhanced accumulation of phosphorylated a-synuclein and elevated b-amyloid 42/40 ratio caused by expression of the presenilin-1 DT440 mutant associated with familial Lewy body disease and variant Alzheimer's disease. *J Neurosci* 2007; **27**: 13092–13097.
25. Okazaki K, Kakita A, Tanaka H *et al.* Widespread ischemic brain lesions caused by vasculopathy associated with neurofibromatosis type 1. *Neuropathology* 2010; **30**: 627–633.
26. Kasuga K, Konno T, Saito K *et al.* A Japanese family with idiopathic basal ganglia calcification with novel *SLC20A2* mutation presenting with late-onset hallucination and delusion. *J Neurol* 2014; **261**: 242–244.
27. Akima M. A morphological study on the microcirculation of the central nervous system. Selective vulnerability to hypoxia. *Neuropathology* 1993; **13**: 99–112.
28. Norman RM, Urich H. The influence of a vascular factor on the distribution of symmetrical cerebral calcifications. *J Neurol Neurosurg Psychiatry* 1960; **23**: 142–147.
29. Smeyers-Verbeke J, Michotte Y, Pelsmaeckers J *et al.* The chemical composition of idiopathic nonarteriosclerotic cerebral calcifications. *Neurology* 1975; **25**: 48–57.
30. Inden M, Iriyama M, Takagi M, Kaneko M, Hozumi I. Localization of type-III sodium-dependent phosphate transporter 2 in the mouse brain. *Brain Res* 2013; **1531**: 75–83.
31. Jensen N, Schrøder HD, Hejbøl EK, Füchtbauer EM, de Oliveira JR, Pedersen L. Loss of function of slc20a2 associated with familial idiopathic basal ganglia calcification in humans causes brain calcifications in mice. *J Mol Neurosci* 2013; **51**: 994–999.
32. Nishimura M, Naito S. Tissue-specific mRNA expression profiles of human solute carrier transporter superfamilies. *Drug Metab Pharmacokinet* 2008; **23**: 22–44.
33. da Silva RJ, Pereira IC, Oliveira JR. Analysis of gene expression pattern and neuroanatomical correlates for SLC20A2 (PiT-2) shows a molecular network with potential impact in idiopathic basal ganglia calcification ("Fahr's disease"). *J Mol Neurosci* 2013; **50**: 280–283.
34. Shibayama H, Kobayashi H, Nakagawa M *et al.* Non-Alzheimer non-Pick dementia with Fahr's syndrome. *Clin Neuropathol* 1992; **11**: 237–250.
35. Kosaka K. Diffuse neurofibrillary tangles with calcification: a new presenile dementia. *J Neurol Neurosurg Psychiatry* 1994; **57**: 594–596.
36. Yokota O, Terada S, Ishizu H *et al.* NACP/alpha-synuclein immunoreactivity in diffuse neurofibrillary tangles with calcification (DNTC). *Acta Neuropathol* 2002; **104**: 333–341.